European Conference on Optical Communication (ECOC) 2022 © Optica Publishing Group 2022

Fibre Type Identification: Alleviating Ambiguities

Emmanuel Seve, Sebastien Bigo, Patricia Layec

Nokia Bell Labs France, Nozay, France, emmanuel.seve@nokia-bell-labs.com

Abstract. *We correlate accumulated dispersions measured in coherent receivers to autonomously identify fibre types in a network without traffic interruption. We propose two techniques to cope with ambiguities: one for ranking solutions by likeliness and one for accelerating their extraction by x100 without enumerating all solutions. ©2022 The Author(s)*

Introduction

To make sure that optical networks operate close to their maximum capabilities, operators need to decrease their "design margins" [1-2]. Various machine learning-based techniques [3-17] have been proposed to decrease design margins through reduction of uncertainty on networks' physical parameters. In this paper, among all sources of uncertainties, we focus on inaccurate fiber type and chromatic dispersion, e.g., from poor inventory, or splicing mistakes. In [18-19], we proposed a technique to autodiscover the fiber type and estimate the chromatic dispersion parameters by correlating the accumulated dispersion (CD) of all established network lightpaths measured by coherent receivers. However, the technique sometimes finds that multiple fiber types could meet all the conditions, especially when network links (i.e., section between two neighbor nodes) are short and when CD measurement uncertainty is high. In this paper, we propose two major enhancements to help process the fiber ambiguities: (1) a method to rank solutions from most to least probable, so that the operators' attention can be brought to likely anomalies in their fiber inventories, (2) a method to accelerate their extraction by x100 without enumerating all solutions.

Method with unknown uncertainty

We propose the following mixed integer linear program (MILP) to predict characteristics (type, chromatic dispersion value and slope) of all links. We made two major improvements with respect to our previous MILP reported in [18-19].

The first one concerns the CD measurement uncertainty, expressed as ΔD^{LP} in [18-19]. It was a fixed value for all the CD measurements, and it was also an input parameter of the MILP. To account for the fact that the CD measurement uncertainty is not always known, we transform it into a variable, and therefore make it an output of the MILP. More specifically, we define two variables for the CD measurement uncertainty: ΔCD_j^{Min} and ΔCD_j^{Max}, representing the lower and upper bounds of the CD measurement uncertainty. These two variables may vary from one generation of transceivers to the next, therefore we introduce as many variables ΔCD_j^{Min} and ΔCD_j^{Max} as the number of lightpaths.

The second improvement benefits to networks where the algorithm returns multiple solutions, i.e., when not all fiber types ambiguities are eliminated. It consists of ranking the solutions by likelihood. To do so, we leverage the first improvement. By making the CD uncertainty an unknown variable, we also introduce the possibility to make the MILP minimize it. We can then sort the solutions by their objective functions in ascending order, the most likely appearing first in a multi-solution search.

Acronyms

CD: accumulated chromatic dispersion, LP: lightpath, L: link

Input parameters

- N^{LP} : number of lightpaths,
- N : number of network links,
- N_f: Number of possible fiber types,
- λ_0 : central wavelength (1550 nm),
- λ_j: wavelength of lightpath *j*,
- $\Theta_{i,j}$: (binary) = 1 if link i is on lightpath j,
- $CD_{j,\,meas}^{LP}(\lambda)$: measured CD for lightpath *j*,
- $CD_i^L(\lambda_0)_{k,\,min/max}$: minimum or maximum CD for link i assuming fiber type *k*.

Output parameters

- $CD_i^L(\lambda_0)$: CD of the link *i* for λ_0,
- $CD'^L_i(\lambda_0)$: CD slope of the link *i* for λ_0,
- $FT_{i,k}$: fiber type (= 1 if link i is of type k),
- $(\Delta CD_j^{Min}, \Delta CD_j^{Max}) > 0$: lower and upper bound of the CD measurement uncertainty.

Constraints (see [19] for more details)

CD for the lightpath *j* ($\forall j \in [1, N^{LP}]$):

$$\sum_{i=1}^{N}\begin{bmatrix} CD_i^L(\lambda_0) \\ +(\lambda-\lambda_0)CD'^L_i(\lambda_0)\end{bmatrix}\Theta_{i,j} \leq CD_{j,\,meas}^{LP}(\lambda)+\Delta CD_j^{Max} \quad (1)$$

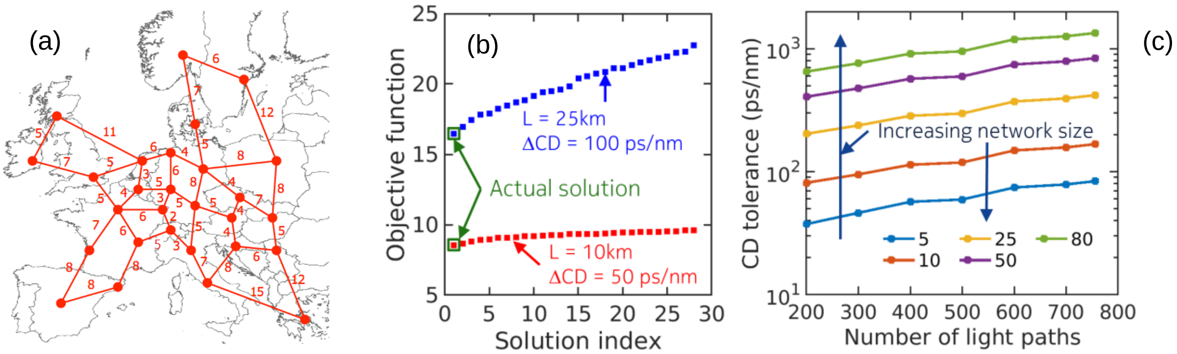

Fig. 1: (a) The European backbone network topology consisting of N = 28 nodes, 41 CD uncompensated links [20], (b) objective function vs solution index, (c) CD tolerance vs the number of lightpaths and the network size.

$$\sum_{i=1}^{N}\begin{bmatrix} CD_i^L(\lambda_0) \\ +(\lambda-\lambda_0)CD'^L_i(\lambda_0)\end{bmatrix}\Theta_{i,j} \geq CD^{LP}_{j,\,meas}(\lambda) - \Delta CD_j^{Min} \quad (2)$$

CD for the link i:

$$\sum_{k=1}^{N_f} CD_i^L(\lambda_0)_{k,\,min}\ FT_{i,\,k} \leq CD_i^L(\lambda_0) \quad (3)$$

$$CD_i^L(\lambda_0) \leq \sum_{k=1}^{N_f} CD_i^L(\lambda_0)_{k,\,max}\ FT_{i,\,k} \quad (4)$$

CD slope for the link i:

$$\sum_{k=1}^{N_f} CD'^L_i(\lambda_0)_{k,\,min}\ FT_{i,\,k} \leq CD'^L_i(\lambda_0) \quad (5)$$

$$CD'^L_i(\lambda_0) \leq \sum_{k=1}^{N_f} CD'^L_i(\lambda_0)_{k,\,max}\ FT_{i,\,k} \quad (6)$$

Single fiber type per link:

$$\sum_{k=1}^{N_f} FT_{i,\,k} = 1,\ FT_{i,\,k} = \{0,1\} \quad (7)$$

Objective function (OF)

$$min\left(OF = \sum_{j=1}^{N^{LP}}\left(\Delta CD_j^{Max} + \Delta CD_j^{Min}\right)/N^{LP}\right) \quad (8)$$

Multi-solutions & ranking

To obtain all fiber types compliant with Eqs (1)-(7), we apply the following procedure. For the first step, we search the first solution ("sol1") while minimizing the objective function (8) which is the sum over all lightpaths of the CD uncertainties (Min and Max) normalized by the number of lightpaths (N^{LP}). We run again the MILP with an additional constraint to push the algorithm to find a new solution "sol 2" different from "sol 1". This "eliminating" constraint is defined as:

$$S = \sum_{i=1}^{N}\sum_{k=1}^{N_f} K_{i,\,k}\ FT_{i,\,k} < N \quad (9)$$

Where $K_{i,\,k}$ is equal to 1 when the link i of the solution "sol 1" is type k and -1 otherwise. The constraint (9) is only satisfied by a solution differing from "sol 1" by at least one link. After each new solution "sol x", we add a xth constraint defined by the inequation (9) using the coefficient $FT_{i,\,k}$ of this xth solution until the moment where there are no solutions satisfying Eqs. (1)-(7) anymore. These solutions are naturally sorted by an ascending value of the objective function which reflects the amount of CD uncertainty according to eq. (8). We consider the European backbone network made of 28 nodes and N = 41 dispersion uncompensated links (Fig. 1(a)). The labels correspond to the length of the links (i.e., segment between two nodes) as a multiple of 80 km, the amplifier span length. The network is based on five fiber types: LS, DSF, LEAF, TL and SSMF with dispersion and dispersion slope values shown in Table 1. We randomize the dispersion of every fiber link in the range shown in the table 1 as in [18-19] to create a realistic set of data. We scaled the network to illustrate the impact of the CD uncertainties for smaller networks. In Fig. 1(b), we plot the objective function as function of the solution rank when the fiber span length (also called network size) is reduced to 10 and 25 km. We process 300 lightpaths (N^{LP}) where further random deviation is added to the monitored CD within ±50 ps/nm and ±100 ps/nm, to account for the measurement inaccuracy. The green square corresponds to the actual solution showing that it has the smallest objective function. As inaccuracy grows, our method shows expected limitations. We define the "CD tolerance" as the level of inaccuracy where the actual function does not come up as #1. Fig 1(c) represents this CD tolerance and is plotted as function of the number of lightpaths. The CD tolerance decreases when the number of lightpaths is smaller as fewer lightpaths share common links. The main impact comes from the network size: the CD tolerance decreases almost proportionally with the network size.

Tab. 1: Fiber dispersion characteristics à 1550 nm from datasheets (D in ps/nm/km, D' in ps/nm^2/km)

	LS	DSF	LEAF	TL	SSMF
D_{min}	-5	-0.7	-2.7	6.2	13.3
D_{max}	-2.4	1	4.8	9.2	18.6
D'_{min}	0.06	0.06	0.074	0.042	0.05
D'_{max}	0.08	0.08	0.093	0.062	0.067

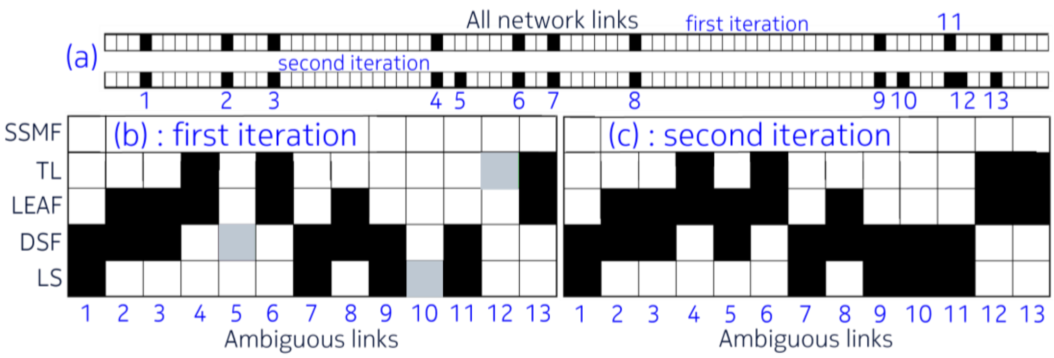

Fig. 2: (a) 13 identified ambiguous links (black squares) among the 82 links after the first (top) and second iteration (bottom). List of fiber types for each ambiguous link for the first (b) and second (c) iteration.

Accelerated ambiguity search

When CD uncertainty is approaching the CD tolerance, the number of solutions returned can be large. The "exhaustive search" method would consist in searching all solutions as presented in the previous paragraph. This method is very time consuming with a high CD uncertainty or small network. We propose a fast method to reach this goal without searching all solutions.

In the exhaustive search, each new solution mainly differs from the previous one by only one link. To accelerate this ambiguity search, we propose to make several simultaneous changes to the previous algorithm. This method starts once the first solution "sol 1" is found and the objective function is then replaced by the sum S. The minimization of S leads to a new solution whose difference with the previous solution is maximized. We also change the way we are affecting the values of $K_{i,k}$, in the constraint (9). At each iteration of the accelerated method, the term $K_{i,k}$, is equal to 1 for all "k" fiber types found in all previous solutions. Fig. 2 illustrates how the list of fiber types is evolving after each iteration of the accelerate ambiguity search method. For that example, we consider the European network scaled to 10km network size with one fiber arrangement and one traffic matrix of 300 lightpaths. The CD uncertainty is equal to 80 ps/nm. For this case, the 13 ambiguous links are found 2 iterations after the first solution is founded. In Fig. 2(a), we represent by black squares the 10 and 13 ambiguous links found after the first and second iteration. Fig. 2(b)(c) show the list of fiber types for the 13 ambiguous links after the first and second iteration. Black squares correspond to the ambiguous fiber types. Links 5, 10 and 12 (grey squares) are not yet identified as ambiguous after the first iteration. The ambiguity is only revealed after the second (and last) iteration. White squares stand for fiber types which do not fulfil the conditions. This way of presenting ambiguous fiber types by black squares can also be viewed as a matrix representation of the terms $K_{i,k}$ in equation (9): +1 for the non-white squares and -1 otherwise. We compared the exhaustive and accelerated method with the same configuration as in Fig. 2 and there is a perfect match between ambiguous links found by the two methods. In Fig. 3, we plot the computation time, the number of solutions and the ambiguous links as a function of the CD uncertainty. The number of solutions can reach 695 (i.e., 13 ambiguous links) for a CD uncertainty of 80 ps/nm. To list all ambiguous links with their possible fiber types, the computation time increases with CD uncertainty (until x100) for the exhaustive method whereas it is almost independent for the accelerated method. This ratio between computation times can even be higher for larger CD uncertainties. The number of iterations being almost constant with the number of ambiguous links.

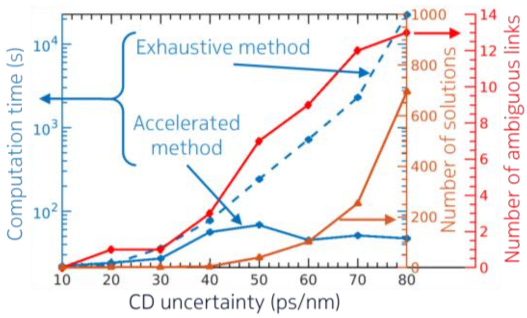

Fig. 3: Computation time of the exhaustive (dashed line) and accelerated method (solid line) vs CD uncertainty. The second and third y-axis displays the number of solutions and ambiguous links, respectively.

Conclusions

By monitoring and correlating the accumulated chromatic dispersion of all network lightpaths, we identify the fiber type of each link. When ambiguities remain, we developed two methods: one to rank all solutions by likeliness and one to accelerate the search by up x100 by identifying ambiguous links without enumerating all solutions. Each link of the network is either completely identified without any ambiguity or the list of possible fiber types is strongly reduced.

References

[1] Y. Pointurier, “Design of low-margin optical networks,” J. Opt. Commun. Netw., Vol. **9**, no. 1, p. A9-A17 (2018).

[2] J-L. Augé, “Can we use flexible transponders to reduce margins?”, Proc. OFC, OTu2A.1 (2013).
E. Seve, J. Pesic, C. Delezoide, S. Bigo and Y. Pointurier, "Learning process for reducing uncertainties on network parameters and design margins," in Journal of Optical Communications and Networking, vol. 10, no. 2, pp. A298-A306, Feb. 2018, doi: 10.1364/JOCN.10.00A298.

[3] P. Soumplis, K. Christodoulopoulos, M. Quagliotti, A. Pagano and E. Varvarigos, "Network Planning with Actual Margins," in Journal of Lightwave Technology, vol. 35, no. 23, pp. 5105-5120, 1 Dec.1, 2017, doi: 10.1109/JLT.2017.2743461.

[4] I. Sartzetakis, K. Christodoulopoulos and E. Varvarigos, "Improving QoT estimation accuracy through active monitoring," 2017 19th International Conference on Transparent Optical Networks (ICTON), 2017, doi: 10.1109/ICTON.2017.8025000

[5] C. Rottondi, L. Barletta, A. Giusti and M. Tornatore, "Machine-learning method for quality of transmission prediction of unestablished lightpaths," in Journal of Optical Communications and Networking, vol. 10, no. 2, pp. A286-A297, Feb. 2018, doi: 10.1364/JOCN.10.00A286.

[6] M. Bouda et al., "Accurate prediction of quality of transmission based on a dynamically configurable optical impairment model," in Journal of Optical Communications and Networking, vol. 10, no. 1, pp. A102-A109, Jan. 2018, doi: 10.1364/JOCN.10.00A102.

[7] G. Liu, K. Zhang, X. Chen, H. Lu, J. Guo, J. Yin, R. Proietti, Z. Zhu and S.J. Ben Yoo, “The First Testbed Demonstration of Cognitive End-to-End Optical Service Provisioning with Hierarchical Learning across Multiple Autonomous Systems,” Proc. OFC, Th4D.7 (2018).

[8] E. Seve, J. Pesic and Y. Pointurier, "Associating machine-learning and analytical models for quality of transmission estimation: combining the best of both worlds," in Journal of Optical Communications and Networking, vol. 13, no. 6, pp. C21-C30, June 2021, doi: 10.1364/JOCN.411979.

[9] T. Sasai, M. Nakamura, S. Okamoto, F. Hamaoka, S. Yamamoto, E. Yamazaki, A. M.H. Nishiszawa and Y. Kisaka, "Simultaneous Detection of Anomaly Points and Fiber Types in Multi-Span Transmission Links Only by Receiver-Side Digital Signal Processing," 2020 Optical Fiber Communications Conference and Exhibition (OFC), 2020.

[10] T. Tanaka, T. Inui, S. Kawai, S. Kuwabara and H. Nishizawa, "Monitoring and diagnostic technologies using deep neural networks for predictive optical network maintenance [Invited]," in Journal of Optical Communications and Networking, vol. 13, no. 10, pp. E13-E22, October 2021, doi: 10.1364/JOCN.424428.

[11] K. Abdelli, H. Griesser, P. Ehrle, C. Tropschug and S. Pachnicke, "Reflective fiber fault detection and characterization using long short-term memory," in Journal of Optical Communications and Networking, vol. 13, no. 10, pp. E32-E41, October 2021, doi: 10.1364/JOCN.423625.

[12] H. Lun et al., "Machine-learning-based telemetry for monitoring long-haul optical transmission impairments: methodologies and challenges [Invited]," in Journal of Optical Communications and Networking, vol. 13, no. 10, pp. E94-E108, October 2021, doi: 10.1364/JOCN.426826.

[13] D. Zibar, A. M. Rosa Brusin, U. C. de Moura, F. Da Ros, V. Curri and A. Carena, "Inverse System Design Using Machine Learning: The Raman Amplifier Case," in Journal of Lightwave Technology, vol. 38, no. 4, pp. 736-753, 15 Feb.15, 2020, doi: 10.1109/JLT.2019.2952179.

[14] N. Morette, I. F. de Jauregui Ruiz, H. Hafermann and Y. Pointurier, "On the Robustness of a ML-based Method for QoT Tool Parameter Refinement in Partially Loaded Networks," 2022 Optical Fiber Communications Conference and Exhibition (OFC), 2022

[15] N. Morette, I. F. de Jauregui Ruiz and Y. Pointurier, "Leveraging ML-based QoT Tool Parameter Feeding for Accurate WDM Network Performance Prediction," 2021 Optical Fiber Communications Conference and Exhibition (OFC), 2021

[16] W. Du, D. Cote, C. Barber and Y. Liu, "Forecasting loss of signal in optical networks with machine learning," in Journal of Optical Communications and Networking, vol. 13, no. 10, pp. E109-E121, October 2021, doi: 10.1364/JOCN.423667.

[17] M. Ruiz, D. Sequeira and L. Velasco, "Deep learning-based real-time analysis of lightpath optical constellations [Invited]," in Journal of Optical Communications and Networking, vol. 14, no. 6, pp. C70-C81, June 2022, doi: 10.1364/JOCN.451315.

[18] E. Seve, C. Delezoide, J. Pesic, S. Bigo and Y. Pointurier, "Automated Fiber Type Identification," In Proceedings IEEE European Conference on Optical Communication (ECOC), 2018, doi: 10.1109/ECOC.2018.8535361.

[19] E. Seve, C. Delezoide, J. Pesic, A. Giorgetti, A. Sgambelluri, N. Sambo, S. Bigo and Y. Pointurier, "Automated Fiber Type Identification in SDN-Enabled Optical Networks," in Journal of Lightwave Technology, vol. 37, no. 7, pp. 1724-1731, 1 April1, 2019, doi: 10.1109/JLT.2019.2896041.

[20] http://sndlib.zib.de/home.action